

## Spray-Flame Dynamics in a Rich Droplet Array

Colette Nicoli · Pierre Haldenwang · Bruno Denet

Received:

**Abstract** : We numerically study spray-flame dynamics. The initial state of the spray is schematized by alkane droplets located at the nodes of a face-centered 2D-lattice. The droplets are surrounded by a gaseous mixture of alkane and air. The lattice spacing  $s$  reduced by the combustion length scale is large enough to consider that the chemical reaction occurs in a heterogeneous medium. The overall spray equivalence ratio is denoted by  $\varphi_T$ , with  $\varphi_T = \varphi_L + \varphi_G$ , where  $\varphi_G$  corresponds to the equivalence ratio of the gaseous surrounding mixture at the initial saturated partial pressure, while  $\varphi_L$  is the so-called liquid loading. To model such a heterogenous combustion, the retained chemical scheme is a global irreversible one-step reaction governed by an Arrhenius

---

Colette Nicoli\* · Pierre Haldenwang

M2P2, UMR-CNRS 7340; CNRS-AMU -Ecole Centrale Marseille

13451 Marseille Cedex 20, France \* Corresponding author

E-mail: : Colette.nicoli@univ-amu.fr

Bruno Denet

IRPHE, Aix-Marseille-Université-CNRS-Ecole Centrale Marseille

13451 Marseille Cedex 20, France

law, with a modified heat of reaction depending on the local equivalence ratio.  $\varphi_T$  is chosen in the range  $0.9 \leq \varphi_T \leq 2$ . Three geometries ( $s = 3, s = 6, s = 12$ ) and four liquid loadings,  $\varphi_L = 0.3, \varphi_L = 0.5, \varphi_L = 0.7, \varphi_L = 0.85$  are studied. In the rich sprays, our model qualitatively retrieves the recent experimental measurements: the rich spray-flames can propagate faster than the single-phase flames with the same overall equivalence ratio. To analyse the conditions for this enhancement, we introduce the concept of "spray Peclet number", which compares the droplet vaporization time with the combustion propagation time of the single-phase flame spreading in the fresh surrounding mixture.

Keywords : droplet combustion · heterogeneous combustion · reduced kinetics · spray-flame · two phase-combustion

## 1 Introduction

Two phase combustion has significant applications when the fuel is injected under liquid phase as in diesel, aerospace engines or furnaces. The present work deals with spray-flame dynamics, for which it is well-admitted that  $\varphi_G$  and  $\varphi_L$  and mean droplet radius are the three most important parameters.  $\varphi_G$ , the gaseous equivalence ratio resulting from the initial saturated mixture of fuel vapour and the air surrounding the pure fuel droplets is controlled by the experimentalists thanks to thermodynamics considerations (i.e the unburnt temperature determines the fuel saturated partial pressure that defines the initial conditions of the spray).  $\varphi_L$  is the liquid loading (or the equivalence ratio resulting from the fuel under liquid phase). As for the mean droplet radius, it results from a complex process of nucleation (or atomization), that includes the skill of the experimentalist.

In the experimental literature, two manners are generally used to present the results: the experimentalist fixes the unburnt temperature and provides us with the data at given  $\phi_G$  [1]. On the other hand, if the experimentalist fixes the amount of fuel under liquid phase (for instance, the pressure drop in the Wilson chamber at the stage of spray formation), the data are presented with fixed  $\phi_L$  [2, 3]. In a recent companion paper [4], we have analyzed the spray dynamics under the first point of view. The present paper considers the second point of view (i.e, fixed  $\phi_L$ ), following the same way of the analyses carried out in [2], [3]. Both points of view are interesting, since each one allows us to put forward particular, and complementary, characteristics on rich spray-flames.

In a general manner, experiments of combustion in sprays at high pressure have revealed behaviors in large departure from the equivalent gaseous premixed flames. For instance, results obtained by Nomura et al. [5] in microgravity have shown that spray-flames in lean ethanol-air mixtures can propagate faster than the equivalent gaseous flames, and slower in globally rich mixtures. Additional contribution by Nomura et al. [6] discussed the role of the droplet size and the liquid loading on spray-flame speed. Recent numerical studies [7, 8] concerning globally lean mixtures with a fixed overall equivalence ratio  $\phi_T = 0.85$  brings complementary results concerning the mixture composition effects and the droplet size influence on spray-flame dynamics. On the other hand, classical ground experiments by Hayashi et al. [1] and Bradley et al. [3] in a Wilson chamber have exhibited opposite observations to the ones made by Nomura et al. [5]: spray-flames in rich mixtures of ethanol (or iso-octane) and air are faster than the equivalent gaseous premixed flame.

The present numerical study aims at extending the previous works [7, 8] for investigating the problem of spray-flames dynamics to globally rich mixtures. More precisely, this consists in schematizing the initial unburnt two-phase medium thanks to a centered 2D-lattice of heavy alkane droplets to estimate the influence of the initial configuration on the spray-flame dynamics.  $s$  denotes the lattice spacing, in such a way that the droplet radius is determined as a function of  $s$  and  $\varphi_L$ . The role of liquid loading is studied for three values of  $s$ . Here, the droplet inter-distance  $s/\sqrt{2}$  in the network -in comparison with the characteristic reaction diffusion scale- is supposed too large for considering that the combustion takes place in a homogeneous medium. In such a configuration,  $\varphi$ , the local equivalence ratio, can vary from a very rich (large) value close the droplets to  $\varphi_G$ . We denote the overall equivalence ratio of the spray by  $\varphi_T$  (with  $\varphi_T = \varphi_G + \varphi_L$ ).

## 2 Modelling for spray-flame

The present spray-flame numerical modelling treats the usual set of conservation laws: mass, momenta, energy and species. Since the accurate chemical schemes for alkane are too complex for efficient simulations, the standard approach for a heterogeneous medium considers a simplified chemical kinetics. The simplest manner consists of choosing an irreversible 1-step reaction, the parameters of which are adjusted to mimic the laminar flame dynamics. It is known that the classical one-step Arrhenius law largely overestimates the adiabatic flame temperature of the rich mixture. To overcome this difficulty to assess the laminar flame speed correctly, we considered an easy modification [9, 10] of the latter chemical scheme: heat release is a linear function  $F(\varphi_u)$  of the fresh premixture equivalence ratio  $\varphi_u$ . Hence, the use of this model in a heterogeneous

mixture needs to estimate  $\varphi_u$ , the "upstream equivalence ratio", thanks to a specific combustion invariant [9, 10] .

$\varphi_T$ , the initial overall equivalence ratio of the fresh spray is chosen in the range  $0.9 \leq \varphi_T \leq 2$  . Four values of liquid loadings are studied:  $\varphi_L = 0.3$  and  $0.6 \leq \varphi_G \leq 1.7$  ,  $\varphi_L = 0.5$  and  $0.4 \leq \varphi_G \leq 1.5$  ,  $\varphi_L = 0.7$  and  $0.2 \leq \varphi_G \leq 1.3$  ,  $\varphi_L = 0.85$  and  $0.05 \leq \varphi_G \leq 1.15$ . The purely gaseous premixed flame is also studied and corresponds to the zero liquid loading  $\varphi_L = 0$  and  $0.9 \leq \varphi_G \leq 2$ . As set out further, the value  $\varphi_G$  is very important for spray-flame dynamics. First, it must be noted that the gaseous premixture surrounding the droplets is not always flammable (i.e when  $\varphi_G \leq 0.5$ ). So, except when  $\varphi_L = 0.3$  where  $0.6 \leq \varphi_G \leq 1.7$ , there are always initial spray compositions in the range  $(0.9 \leq \varphi_T \leq 2)$  where the surrounding gaseous premixture is too lean to be flammable (i.e when  $(\varphi_L \geq 0.5)$  and  $[\varphi_T - \varphi_L \leq 0.5]$  ). The lattice spacing value also influences the spray dynamics: three normalized values of  $s$  are retained ( $s = 3, s = 6, s = 12$ ).

## 2.1 Non-dimensioning

Non-dimensioning is performed with the use of the theoretical data related the stoichiometric (gaseous) premixed flame as derived in the theoretical papers by Joulin and Mitani [11] and Garcia-Ybarra et al [12]. We define the stoichiometric flame temperature, as  $T_b^*$  , given by

$$T_b^* = T_u + \frac{(Y_f)_u^* Q}{C_p v_f M_f}$$

Temperature and species mass fractions are handled under the reduced forms

$$\theta = (T - T_u) / (T_b^* - T_u) ; \psi_i = Y_i / Y_{i,u}^*$$

( $i = f$  for the alkane and  $i = o$  for oxygen).

The subscript "u" is associated with the fresh mixture, at the temperature  $T_u$ . The subscript "b" is associated with the burnt mixture, at the flame temperature  $T_b$ . The superscript "\*" is associated with the stoichiometric values. As for the time and length scales, we use  $D_{th,b}^*$ , the thermal diffusivity coefficient of the burnt gases, and the stoichiometric (gaseous) flame speed given by

$$(U_L^*)^2 = \frac{4}{Ze^3} \left( \frac{\rho_b^*}{\rho_u^*} \right)^2 D_{th,b}^* \left[ (\rho_b^*)^2 \nu_f M_f Y_{o,u}^* B_b \right] \exp(-T_A/T_b^*)$$

This allows us to establish the scalar conservation laws as follows

$$\frac{\partial \theta}{\partial t} + \bar{V} \cdot \bar{\nabla} \theta = \frac{1}{\rho C_p} \text{div}(\lambda \bar{\nabla} \theta) + F(\varphi_u) W(\rho, \psi_i, \theta)$$

$$\frac{\partial \psi_i}{\partial t} + \bar{V} \cdot \bar{\nabla} \psi_i = \frac{1}{\rho} \text{div}(\rho D_i \bar{\nabla} \psi_i) - \nu_i M_i W(\rho, \psi_i, T)$$

where the reaction rate (thereafter called production term) is now defined under dimensionless form as

$$W(\rho, \psi_i, \theta) = \frac{Ze^3}{4} \left( \frac{\rho_u^*}{\rho_b^*} \right)^2 \psi_f \psi_o \left[ \frac{\rho}{\rho_b^*} \right]^3 \exp \left[ Ze \frac{\theta - 1}{1 + \gamma(\theta - 1)} \right]$$

with the Zeldovich number,  $Ze = T_A(T_b^* - T_u) / (T_b^*)^2$  and the thermal expansion parameter  $\gamma = (T_b^* - T_u) / T_b^*$ .  $T_A$  is the reduced activation energy.  $\rho$  is the density of the mixture.

The overall equivalence ratio of the spray is given by the ratio of the total amount of fuel to the total amount of oxygen in the lattice.

$$\varphi_T = \frac{\nu_o M_o}{\nu_f M_f} \frac{\int_{\text{initial-lattice}} \rho_f dv}{\int_{\text{initial-lattice}} \rho_o dv}$$

while the quantity  $\varphi_L$  [resp.  $\varphi_G$ ] only takes account of the fuel density under liquid phase [resp. gas phase].

### 3 Heterogeneous Medium and Combustion model

Because combustion spreads in a medium of variable composition, a chemical scheme taking account of the variable equivalence ratio of the mixture is required. To be numerically efficient, the chemical scheme must be of minimal complexity. We turned towards chemical schemes that are founded on an irreversible one-step reaction governed by an Arrhenius law. We retain the kinetic scheme [9] recently developed for octane-air mixtures. Metastable species present in the burnt gases are considered. The heat of reaction is evaluated to retrieve the true adiabatic flame temperature. It turns out that the procedure leads us to a good agreement with the experimental data on gaseous premixed flame speed [9, 10]. The general form given to the adjustment appears in the energy conservation law, where a heat release depending on the equivalence ratio in the fresh mixture has introduced by the multiplication by the following factor

$$F(\varphi_u) = [1 - \alpha(\varphi_u - 1)] \text{ if } \varphi_u \in [0.5, 2]$$

whereas  $W = 0$  if  $\varphi_u \notin [0.5, 2]$

where  $\varphi_u$  is a characteristic quantity related to the flamelet theory that is defined below and  $\alpha$  is a coefficient depending on the fuel. The Zeldovich number determined theoretically appears as independent of the equivalence ratio. For octane-air premixture we obtained  $\alpha = 0.33$  and  $Ze = 7$  [9].

The above-mentioned flamelet model considers the spray-flame as series of connected premixed flames which have their own dynamics. This dynamics results from a kinetic model that has been developed for purely gaseous premixed flames. In this context,  $\varphi_u$  is nothing but the fresh gaseous equivalence ratio upstream the flamelet . In the reference [4] , it is shown how  $\varphi_u$  is derived from two mixture variables. Lastly, as in the conservation laws appears the velocity field , the reaction diffusion

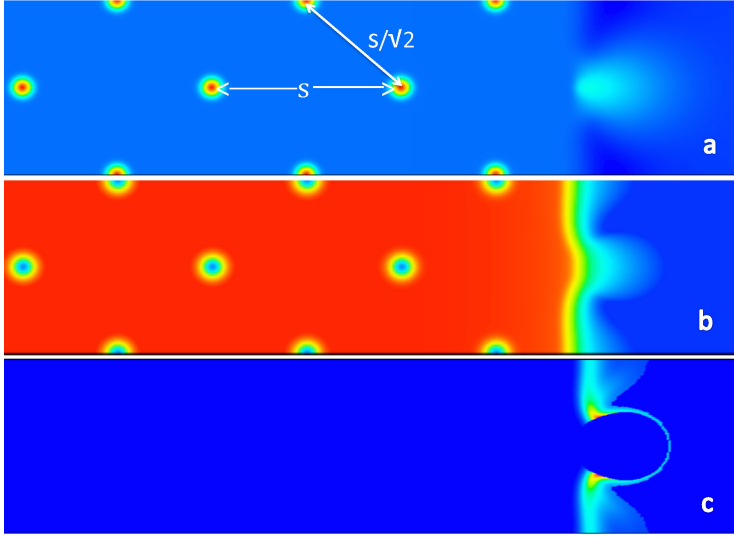


Fig. 1 Alkane air mixture:  $\varphi_T = 1.2$ ,  $\varphi_G = 0.7$ ,  $\varphi_L = 0.5$ ,  $s = 6$ . Three snapshots of the centered 2D- lattice soon after ignition at the right-hand side, a) Fuel mass fraction, a) Oxygen mass fraction c) Field of production term (in color) [flame propagates from right to left].

system is coupled with the Navier-Stokes equations. The overall scheme that computes the Navier-Stokes equations has previously been described in Denet and Haldenwang [13].

### 3.1 Results: Spray-Flame spreading

The numerical simulations have been carried out using the following parameters: the Lewis numbers of fuel, oxygen and nitrogen are respectively  $Le_F = 1.8$ ,  $Le_O = 0.9$ ,  $Le_N = 1$ . Let us recall that the overall equivalence ratio  $\varphi_T$  is varied in the range  $[0.9, 2]$ . The high-level of the non- homogeneity in a spray-flame and the complexity of the spreading are illustrated in figures 1, 2, 3 and 4, which will be commented below.

The numerical simulations concern 2D sprays where the droplets are conceived as very dense pockets of pure fuel, initially located at the node of a face-centered lat-



tice. Equations are solved using mixed finite differences in the longitudinal (spreading) direction / spectral Fourier method in the periodic (transverse) direction. Typical discretization is 3072 nodes in the x-direction and 256 Fourier modes in the y-direction with a time step  $10^{-3}$  in non-dimensional units. These points are developed in the previous papers [4, 7].

More precisely, figure 1 shows three important fields when two triple flames get around the first fuel droplet. Each of these fields are then followed in time : fuel mass fraction is represented in figure 2 , oxygen mass fraction is illustrated in figure 3 and production term is drawn in figure 4 .

These figures concern a rich spray of global equivalence ratio  $\phi_T = 1.2$  with a lean and flammable surrounding gaseous mixture  $\phi_G = 0.7$ . Due to the presence of hot burnt gases, a large dilation of fuel -and oxygen- occurs. Gas expansion creates a very rich stratified premixture that replaces the pure fuel droplet. Figure 2 shows the "vaporization" and the consumption of the first droplet . Simultaneously with fuel vaporization and local heating, the oxygen mobility increases as indicated in figure 3 and creates a premixture in which triple flames propagate accordingly with figure 4, where the production term is plotted.

Figure 4 follows the triple flames that surround the droplet. Their rich wing slowly propagates towards the droplet through an increasingly rich premixture. As for the lean wing, it propagates towards the next droplet with the velocity of a premixed flame with the equivalence ratio  $\phi_G = 0.7$ . Behind this lean flame, there is an oxygen pocket left, around which a diffusion flame can exist [4]. The last picture exhibits the slow combustion of a spherical premixed rich pocket (and not a diffusion flame) that consumes the remaining oxygen contained in the droplet vicinity. As the spray is globally rich,

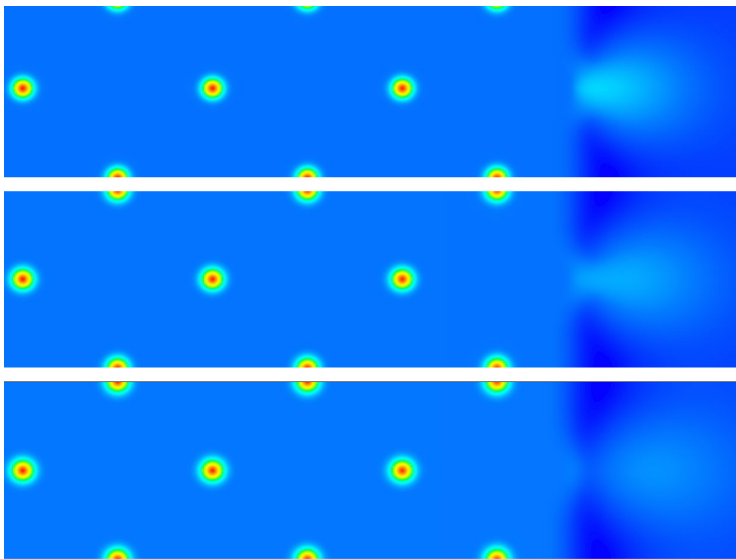


Fig. 2 Fuel mass fraction at three instants after ignition (alkane-air spray:  $\varphi_T = 1.2$  ,  $\varphi_G = 0.7$ ,  $\varphi_L = 0.5$ ,  $s = 6$ )

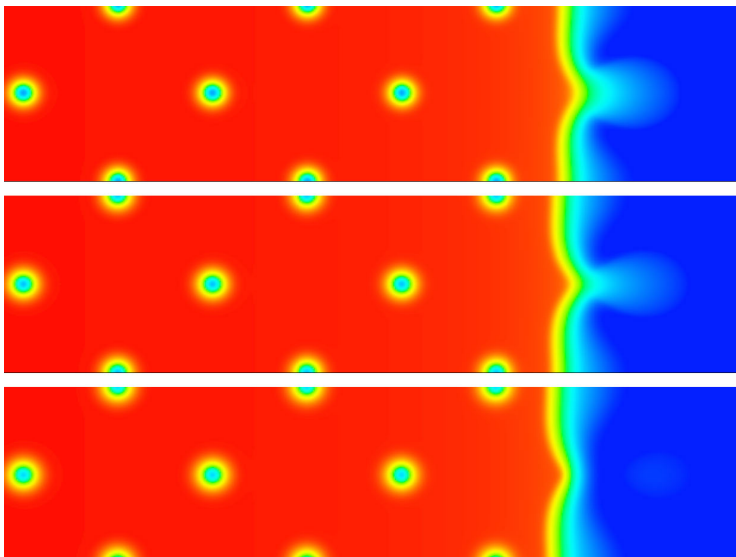


Fig. 3 Oxygen mass fraction at three instants after ignition (alkane-air spray:  $\varphi_T = 1.2$  ,  $\varphi_G = 0.7$ ,  $\varphi_L = 0.5$ ,  $s = 6$ )

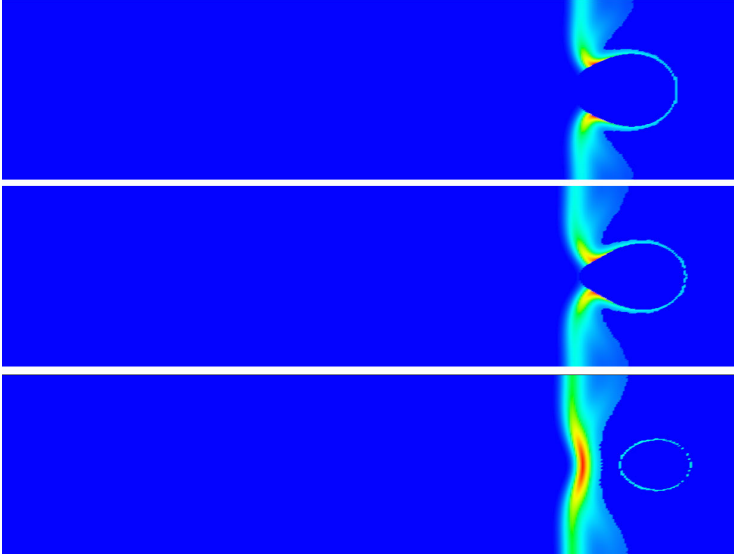


Fig. 4 Production term at three instants after ignition (alkane-air spray:  $\varphi_T = 1.2$ ,  $\varphi_G = 0.7$ ,  $\varphi_L = 0.5$ ,  $s = 6$ )

no oxygen remains in the burnt gases.

Spray-flame speed is deduced from the former leading flame, i.e. from the time required to contaminate several droplets of the lattice. In a general manner, combustion spreading is found to be not uniform in time: it combines stages of vaporization and stages of flame propagation [7]. The spray-flame speed is assessed by following a given isotherm as in [7]. In each studied configuration, the retained non-dimensional isotherm used to follow the leading flame is  $T = 0.65$ . The resulting velocity, normalized by the stoichiometric premixed flame speed, is plotted in Fig. 5 (respectively Fig. 6 and 7) in the plane overall equivalence ratio- spray-flame speed for the given lattice spacing  $s = 3$  (resp.  $s = 6$ ,  $s = 12$ ) and various liquid loadings ( $\varphi_L = 0$ ), ( $\varphi_L = 0.3$ ), ( $\varphi_L = 0.5$ ), ( $\varphi_L = 0.7$ ), ( $\varphi_L = 0.85$ ). In Figures 5-6-7, the spray-flame speed dependences with the overall equivalence ratio are highly different if the lattice spacing is small or large.

First of all, note that, if the lattice spacing is  $s = 3$ , the distance between each droplet ( $s/\sqrt{2} = 2.12$ ) is of the same order as the flame thickness. The cold droplets adjacent to the ignited droplet are close enough to be into the direct sphere of influence of the burning droplet, and a rapid contamination by combustion arises. By contrast, for the largest lattice spacing  $s = 12$ , the distance between each droplet equal to  $s/\sqrt{2} = 8.48$  is too large to receive a rapid heating from the neighbor droplets. A purely gaseous flame in stratified mixture must develop to allow the spray-flame propagation.

In figure 5, the normalized spray-flame speeds  $U_s$  dependent on the overall equivalence ratio  $\phi_T$  are drawn, for the smallest lattice spacing  $s = 3$  and various given liquid loadings  $\phi_L$ . It can be observed that whatever the retained liquid loading, the curve of the spray-flame speed in the plane  $(\phi_T, U_s)$  presents a maximum associated to an overall equivalence ratio smaller than  $\phi_T = 1.35$ . The values of the maxima of  $U_s$  are smaller than the maximum  $(\phi_T = 1.05; U_L = 1)$  of the purely gaseous case ( $\phi_L = 0$ ). The smaller the value of  $\phi_L$ , the smaller  $\phi_T$  associated to the maximum speed  $U_s$ : the corresponding value of the spray-flame speed is larger for smaller  $\phi_L$ . When the lattice spacing is small, the droplet radius varies slowly with the liquid loading (see Fig. 8). Droplet radii are small, nevertheless, the liquid loading value has an influence on the spray-flame speed as long as the overall equivalence ratio is smaller than 1.35. For greater values of  $\phi_L$ , droplets are bigger and the gaseous surrounding mixture is leaner. The spray-flame speed is slower. Some liquid fuel does not participate in the combustion propagation and the effective equivalence ratio appears leaner than the true overall equivalence ratio of the mixture. In figure 5, all the curves pass through the point  $(\phi_T = 1.35, U_s = 0.725)$ , nearly. Two different behaviors of the spray dynamics compared to the purely gaseous flame (corresponding to  $\phi_L = 0$ ) exist. When

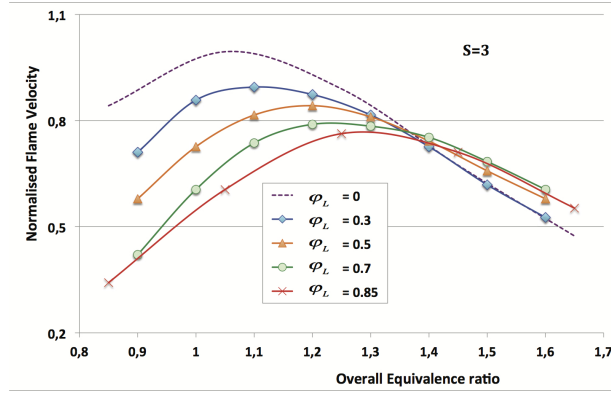


Fig. 5 Spray-flame speed versus overall equivalence ratio of the spray for various liquid equivalence ratios ( $s = 3, 0.9 \leq \phi_T \leq 1.6$ ), iso-octane/air spray

the overall equivalence ratio of the spray is lower than 1.35, the spray-flame spreads always more slowly than the purely equivalent gaseous premixed flame. For larger liquid loading, the spray-flame speed is smaller. Let us recall that when  $\phi_T$  is small there is always a range of gaseous equivalence ratio where the surrounding mixture is not flammable. For higher liquid loading, the range of non-flammable surrounding is larger. When the value of  $\phi_T$  is lower than 1.35, the combustion needs to increase the gaseous equivalence ratio: it is necessary to vaporize the fuel under liquid phase to allow the combustion. The larger the liquid loading is, the more important the quantity of the liquid fuel to vaporize is. This explains why the spray-flame propagates slowly at higher  $\phi_L$  values.

When  $\phi_T \geq 1.35$ , the spray-flame propagates more rapidly than the premixed flame, except for  $\phi_L = 0.3$  where droplets are sufficiently small to rapidly vaporize and contribute completely to the flame propagation (the spray-flame dynamics at  $\phi_L = 0.3$  is

roughly the same as  $\varphi_L = 0$ ). In the other cases,  $\varphi_L \geq 0.5$ , droplet radii are greater, spray-flames are faster because some fuel must remain under liquid phase and does not contribute to the combustion. The spray-flame speed does not vary a lot, the velocity is slightly greater for larger  $\varphi_L$ .

When the lattice spacing is widened, droplets are bigger and further away from the others: for each given mixture composition, more time is necessary to flame propagation from one droplet to the next and to vaporize the liquid fuel. Note that the purely gaseous flame speed depends only on the overall equivalence ratio, but not on the lattice spacing value.

For the intermediate lattice spacing  $s = 6$ , the spray-flame speed  $U_s$  dependence with the overall equivalence ratio is drawn in figure 6. For every liquid loading, the maximum of the curve is shifted towards the right, i.e towards larger overall equivalence ratio (by comparison with the case  $s = 3$ ). As the lattice spacing is larger, the droplet radius is larger and droplet vaporization, fuel diffusion and "mixture creation" last longer. For  $\varphi_L = 0.7$ , a small change in slope is observed for  $\varphi_T = 1.2$  that is the smallest overall equivalence ratio corresponding to a flammable surrounding mixture ( $\varphi_G \geq 0.5$ ). It must be noted that the overall equivalence ratio for which the spray-flame becomes faster than the premixed gaseous flame is different for each  $\varphi_L$  and increases with the liquid loading. In addition, at a given very rich overall equivalence ratio ( $\varphi_T \geq 1.7$ ), the larger liquid loading, the faster spray-flame propagation. For the intermediate lattice spacing  $s = 6$ , droplets presence boosts flame speed for richer sprays. The spray-flame speed curves associated with the intermediate lattice spacing  $s = 6$  shows behaviors intermediate between those observed for the small lattice spacing in figure 5 and those corresponding to the large lattice in figure 7.

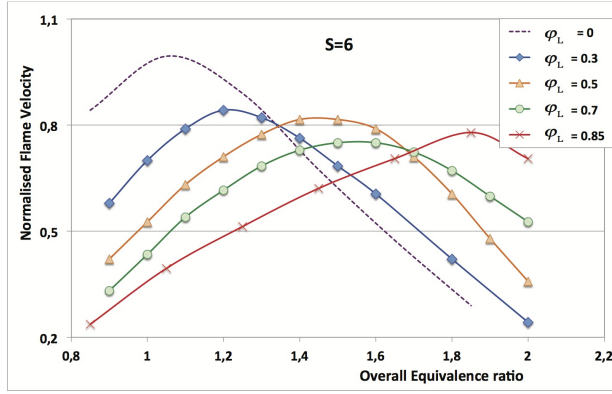


Fig. 6 Spray-flame speed versus overall equivalence ratio of the spray for various liquid equivalence ratios ( $s = 6, 0.9 \leq \varphi_T \leq 1.6$ ), iso-octane/air spray

In figure 7, corresponding to the large lattice spacing  $s = 12$ , it can indeed be observed that the maximum of each curve is shifted towards the right compared with those of the case  $s = 6$ . More precisely, when  $s = 12$ , the maximum of the spray-flame speed is associated with an overall equivalence ratio corresponding to  $(\varphi_T = 1.05 + \varphi_L)$ .  $\varphi_T = 1.05$  is the overall equivalence ratio for the maximum associated with the purely gaseous flame. When  $s = 12$ , the fuel under the liquid phase does not seem to contribute to spray-flame propagation. For the largest lattice spacing, the spray-flame spreads at the speed of the gaseous flame with an effective overall equivalence ratio  $\varphi_G = \varphi_T - \varphi_L$ . Only the maximum value of the spray-flame speed slightly increases with the liquid loading to reach the gaseous value for the largest liquid loading.

Additional informations can be obtained from the order of magnitude of the droplet radii. It must be recalled that the knowledge of the lattice spacing  $s$  and the liquid loading  $\varphi_L$  allows the droplet radius determination. In figure 8, the ratio of the droplet

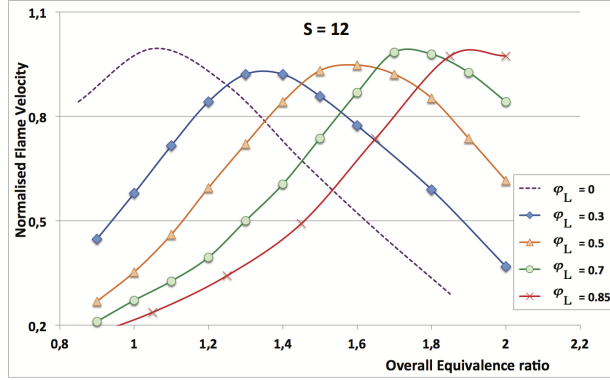


Fig. 7 Spray-flame speed versus overall equivalence ratio of the spray for various liquid equivalence ratios ( $s = 12, 0.9 \leq \phi_T \leq 1.6$ ), iso-octane/air spray

radius  $R_d$  to the lattice spacing  $s$  appears as a function of the liquid loading  $\phi_L$  only. In the same figure, the droplet radius  $R_d$  in the stoichiometric flame length units is drawn in the plane  $(\phi_L, R_d)$  for each lattice spacing studied.

When the lattice spacing is small ( $s = 3$ ), droplet radii are of the order of the reaction zone thickness (i.e flame thickness over the Zeldovich number): almost all the fuel under liquid phase can contribute to the reaction. Combustion propagates in a stratified mixture of the thickness of the lattice spacing (i.e the flame thickness order). For intermediate lattice spacing ( $s = 6$ ), the order of magnitude for the droplet radii is the half of the flame thickness. The vaporization time remains small; it nevertheless becomes four time greater than for the case ( $s = 3$ ), as the propagation time (i.e the time to go from a droplet to the next) is only twice time larger than for ( $s = 3$ ), the spray-flame speed has the same order of magnitude than the spray-flame velocity for the case ( $s = 3$ ), with a maximum slightly smaller observed for an overall equivalence



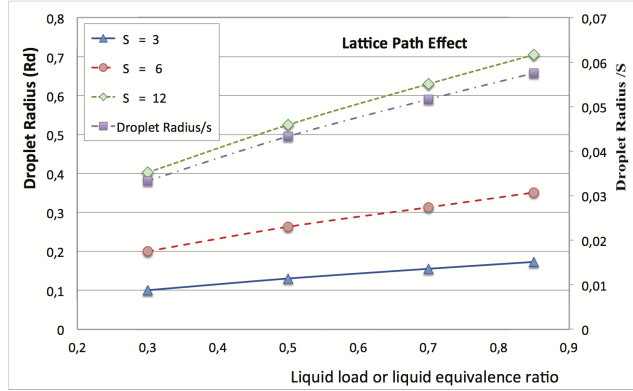


Fig. 8 Normalized Droplet radius versus liquid equivalence ratio of the spray for various lattice spacing ( $s = 3, s = 6, s = 12$ ), iso-octane/air spray

ratio shifted to the right. Only a part of the liquid fuel contributes to the spray-flame spreading after a mixing time in the lattice on the same order of the vaporization time. For large lattice spacing ( $s = 12$ ), it can be observed in figure 8 that droplet radii are of the order as the stoichiometric flame thickness, especially at large liquid loading. As soon as the surrounding gaseous mixture is flammable, the spray-flame can go from one droplet to another. Droplets are too far from each other to feel the influence of the neighboring droplets. The spray-flame behaves as a pure gaseous flame ignoring the presence of droplets.

The behavior of the spray-flame in comparison with the equivalent gaseous flame (in terms of the overall equivalence ratio) can furthermore be qualitatively analyzed for rich mixtures by studying the "spray Peclet number" defined as the ratio of the droplet vaporization time  $\tau_{vap} \propto (\rho_u/\rho_b)/D_{th,b}^* (2R_d)^2$  to the propagation time  $\tau_{prop} \propto$

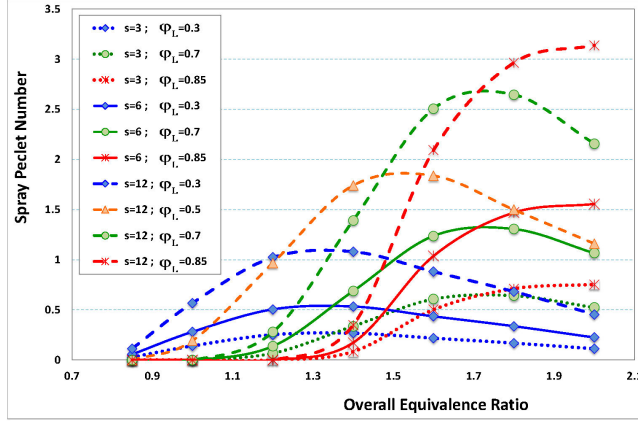


Fig. 9 Peclet Number versus overall equivalence ratio of the spray for various lattice spacing ( $s = 3, s = 6, s = 12$ ), iso-octane/air spray

$s/U_L(\varphi_G)$ . This number can be written as

$$Pe \propto (\rho_u/\rho_b)/D_{th,b}^* (2R_d)^2 / s * U_L(\varphi_G)$$

Various spray Peclet numbers are drawn in figure 9 as a function of the overall equivalence ratio  $\varphi_T$  for various lattice spacings  $s$  and liquid loadings  $\varphi_L$ . It must be noted that, for given  $\varphi_G$  and  $\varphi_L$ , spray Peclet number is in the direct ratio of the lattice spacing (e.g. for  $s = 6$ ,  $Pe$  is twice greater than for  $s = 3$ ).

For the small lattice spacing  $s = 3$ , all Peclet numbers are found small for every  $\varphi_L$ . In this case, figure 5 indicates that the spray-flame speed is found slower than the gaseous flame speed, excepted at high  $\varphi_T$ , for which  $Pe$  concomitantly becomes slightly more significant.

For intermediate lattice spacing  $s = 6$ , Peclet numbers remain small as long as  $\varphi_T < 1.4$ . For richer spray mixture ( $\varphi_T > 1.4$ ) and larger  $\varphi_L$ , the (rich) propagation time becomes sufficiently small to allow a spray-flame faster than the gaseous flame, as

indicated in figure 6 when  $\varphi_T \geq 1.4$ . As the vaporization time is slightly greater than the propagation time, the analysis in Peclet number confirms that a small quantity of fuel remains under liquid phase and does not participate to spray propagation.

For the large lattice spacing  $s = 12$ , the Peclet number becomes larger than one for large  $\varphi_T$ : the propagation time is smaller than the vaporization time. In terms of spray-flame propagation, it corresponds in figure 6 to a velocity always larger than the gaseous flame speed as soon as  $\varphi_T$  becomes larger than a threshold value that depends on  $\varphi_L$ . In other words, as the droplets vaporize owing to flame heating, their evaporation still occurs as the flame has already crossed the current droplet and is propagating towards the next droplet. In such a way that the fuel under liquid phase has no time to contribute to spray propagation. For  $s = 12$ , this mechanism is always correct for rich mixture and high liquid loading. A large spray Peclet number is a marker of this mechanism. It explains why the maximum value of the spray-flame speed is the same as the one of the gaseous flame (i.e. obtained for  $\varphi_T = \varphi_G = 1.05$ ) and happens for ( $\varphi_T = 1.05 + \varphi_L$ ), and why every curve in figure 7 is in translation from each other.

#### 4 Conclusion

Spray-flame propagation in rich situations has been analyzed using a simple combustion model for heterogeneous media. Even if rich spray combustion is rarely desired in practical applications, this situation is nevertheless encountered close to the devices of fuel injection. We have investigated the role of three important parameters: the liquid loading, the overall equivalence ratio, and the mean droplet interdistance (or, equivalently, the droplet radius, both quantities being in link with the spacing of the lattice where the droplets are initially positioned).

Ealier experimental approaches have put forward the particular roles played by liquid loading and droplet size. The present numerical approach was able to vary both parameters, independently. It has hence been possible to determine several domains where the dynamics of spray-flames deeply differs from that of gaseous premixed flames. The mechanisms involved in the non-intuitive observations carried out by the experimentalists about spray-flames have been identified.

In a general manner, droplet vaporization and subsequent fuel mixing helps propagation when needed. We have however put forward a simple criterion for which this general feature does not occur. More precisely, we have proposed to inspect the value of a peculiatr number, called "spray Peclet number", which is the ratio of the droplet vaporization time to the propagation time of the gaseous flame corresponding the combustion of the initial premixture surrounding the droplets. When the spray Peclet number is larger that one, we have established that droplet vaporization does not play any role in the spray-flame propagation. As a result, on the rich side, spray-flame speed is always faster than the gaseous flame.

On the other hand, when the spray Peclet number is small (often zero), droplet vaporization plays a major role. In the different rich cases we have investigated, the spray-flame always spreads more slowly than the equivalent gaseous flame. As for the intermediate values of spray Peclet number (say  $0.3 < Pe < 1$ ), the discussion becomes more intricate. We can nevertheless say that both flames propagate with rates on the same order of magnitude.

In other words, comparing droplet vaporization and single-phase flame propagation discarding liquid loading led us to an effective criterion for explaining why the rich spray-flame becomes faster (or slower) than the gaseous flame of equivalent composition.

## 5 Acknowledgements

The present work has received the support of the Research Program " Micropesanteur Fondamentale et Appliquee " - GDR 2799 - CNRS/CNES under the contract CNES/140569.

## 6 Compliance with Ethical Statements

Funding : this study was funded by a support of the Research Program " Micropesanteur Fondamentale et Appliquee " - GDR 2799 - CNRS/CNES under the contract CNES/140569.

Conflict of Interest: The authors declare that they have no conflict of interest.

## References

1. S. Hayashi, S. Kumagai, and T. Sakai. Propagation velocity and structure of flames in droplet vapor air mixtures. *Combust. Sci. and Tech.*, 15:169–177, 1976.
2. R. Thimothée, C. Chauveau, F. Halter, and I. Gokalp. Characterization of cellular instabilities of a flame propagating in an aerosol.. *Proceedings of ASME Turbo Expo 2015: Turbine Technical Conference and Exposition GT2015*, 6 2015.
3. D. Bradley, M. Lawes, S.Y. Liao, and A Saat. Laminar mass burning and entrainment velocities and flame instabilities of isooctane, ethanol and hydrous ethanol/air aerosols. *Combust. and Flame*, 161(6):1620–1632, 2014.
4. C. Nicoli, B. Denet, and P. Haldenwang. Rich spray-flame propagating through a 2d-lattice of alkane droplets in air. *Combust. and Flame*, accepted, 2015.

5. H. Nomura, M. Koyama, H. Miyamoto, Y. Ujiie, J. Sato, M. Kono, and S. Yoda. Microgravity experiments of flame propagation in ethanol droplet vapor air mixture. *Proc. Combust. Inst.*, 28:999–1005, 2000.
6. H. Nomura, I. Kawasumi, Y. Ujiie, and J. Sato. Effects of pressure on flame propagation in a premixture containing fine fuel droplets. *Proc. Combust. Inst.*, 31:2133–2140, 2007.
7. C. Nicoli, B. Denet, and P. Haldenwang. Lean flame dynamics through a 2d lattice of alkane droplets in air. *Combust. Sci. and Tech.*, 186(2):103–119, 2014.
8. C. Nicoli, P. Haldenwang, and B. Denet. Numerical study of flame dynamics through a 2d-lattice of alkane droplets in air. *ECM2013: 6th European combustion meeting*. Lund, Sweden, 6 2013.
9. C. Nicoli and P. Haldenwang. Analysis of one-step chemistry models for flame propagation in various equivalence ratio premixtures of high alkane-air. *SPEIC10: Towards Sustainable Combustion*, Tenerife, 6 2010.
10. C. Nicoli, P. Haldenwang, and B. Denet. Numerical study of spray flames dynamics through a 2d-lattice of droplets in alkane-air mixtures. *SPEIC14: Towards Sustainable Combustion*, Lisboa, 11 2014.
11. G. Joulin and J. Mitani. Linear stability analysis of two-reactant flames. *Combust. and Flame*, 40:235–246, 1981.
12. P. Garcia-Ybarra, C. Nicoli, and P. Clavin. Soret and dilution effects on premixed flames. *Combust. Sci. and Tech.*, 42:235–246, 1984.
13. B. Denet and P. Haldenwang. A numerical study of premixed flames darrieus-landau instability. *Combust. Sci. and Tech.*, 104:143–167, 1995.